Lanthanide Coordination Polymer Nanoparticles for Sensing of Mercury(II) by Photoinduced Electron Transfer

Hongliang Tan, Baoxia Liu, and Yang Chen*

State Key Laboratory of Bioelectronics, School of Biological Science and Medical Engineering, Southeast University, Nanjing, 210096, People's Republic of China

ABSTRACT The metal–organic coordination polymers at the nanoscale have emerged as attractive nanomaterials due to their tunable nature. In this work, we for the first time prepared an adenine-based lanthanide coordination polymer nanoparticle (CPNP) with fluorescence sensing function. This kind of CPNP was composed of adenine, terbium ion (Tb^{3+}), and dipicolinic acid (DPA) as an auxiliary linking molecule that can sensitize the fluorescence of Tb^{3+}. The fluorescence of the CPNPs is very weak due to the existence of photoinduced electron transfer (PET) from adenine to DPA, which prevents the intramolecular energy transfer from DPA to Tb^{3+}, leading to the quench of fluorescence of the CPNPs. In the presence of Hg^{2+}, however, significant enhancement in the fluorescence of CPNPs was observed because of the suppression of the PET process by the coordination of Hg^{2+} with adenine. As a kind of Hg^{2+} nanosensor, the CPNPs exhibit excellent selectivity and ultrahigh sensitivity up to the 0.2 nM detection limit. The CPNPs also possess an approximately millisecond-scale-long fluorescence lifetime due to the inclusion of Tb^{3+} ions. We envision that the CPNPs could find great potential applications in ultrasensitive time-resolved fluorometric assays and biomedical imaging in the future owing to their long emission lifetimes, excellent dispersion, and stability in aqueous solution.

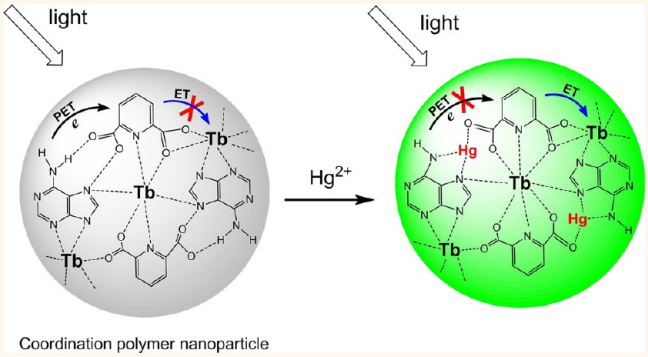

KEYWORDS: coordination polymer nanoparticles · photoinduced electron transfer · Hg^{2+} · sensors

Materials at the nanoscale are of great interest for a wide range of applications in materials and life sciences as well as for medical diagnostics; developing new types of nanomaterials has been the focus of many scientific investigations. In particular, nanoscale coordination polymers (NCPs) built from the association of metal ions and bridging organic ligands have attracted much attention for their tunable nature. The variety of metal ions, organic linkers, and structural motifs affords an essentially infinite number of possible combinations. The NCPs possess potential advantages over conventional organic or inorganic nanomaterials, such as structural and chemical diversity, high loading capacity, and intrinsic biodegradability.[1] One of the most interesting behaviors of the NCPs is their luminescent properties.[2] To date, the NCPs have been examined for their potential applications in gas storage and separation,[3,4] heterogeneous catalysis,[5,6] molecular reorganization and sensing,[7,8] biomedical imaging,[9–11] ion exchange,[12] and drug delivery.[13,14] Nevertheless, most studies of NCPs focus on their exceptional porosity and luminescent properties, and less work on using NCPs as fluorescent probes for sensing of ions or molecules, especially sensing in aqueous solution, was reported.[15–17] Challenges still remain in the design of functional NCPs. Many potential functions and applications of NCPs require them to be constructed from initial building blocks that are environmentally and biologically compatible.[18] Moreover, the sizes of coordination polymers must be carefully controlled to be uniform and below several hundred nanometers for applications in the field of biomedicine.[19] Biomolecules can serve as building blocks to meet these requirements because biomolecules are from nature, mostly

* Address correspondence to yc@seu.edu.cn.

Received for review June 21, 2012 and accepted November 2, 2012.

Published online November 02, 2012
10.1021/nn304469j

© 2012 American Chemical Society

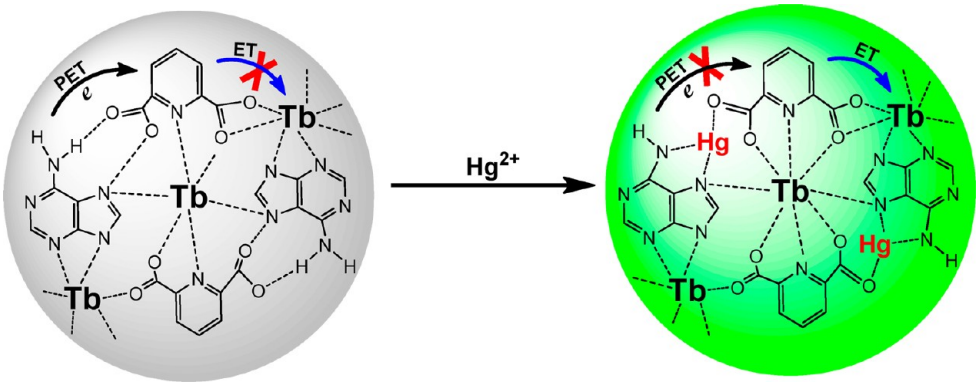

Scheme 1. Coordination Polymer Nanoparticle Ad/Tb/DPA for Sensing of Hg^{2+} by Photoinduced Electron Transfer

water-soluble, and have diverse structures, many binding sites for metal ions, and intrinsic self-assembly properties.[20] The combination of biomolecules could provide NCPs some new properties that cannot be accessed using the simple organic linkers as building blocks and hence have promise for a wider scope of utility. Recently, the Kimizuka group prepared a series of nanoscale coordination polymers using water-soluble nucleotides and lanthanide ions.[10,21−23] These polymers not only can serve as a potent magnetic resonance imaging (MRI) contrast agents but exhibited surprising properties of adaptive encapsulation for guest molecules in the course of self-assembly. The encapsulation of suitable factors can make up for the insufficiency of very low extinction coefficients of lanthanide ions and sensitize the fluorescence of coordination polymers.

Adenine is one of nucleobases that constitute nucleic acids. The characteristics of adenine including accessible lone pair electrons at the nitrogen atom, rich metal binding and H-bonding sites, and the rigidity of the molecular structure make it an ideal building block for constructing metal−organic coordination polymers.[20] Some adenine-based metal−organic coordination polymers have been reported in recent years.[24−28] An and coworkers have prepared several adenine-based metal−organic coordination polymers by employing Zn(II) and Co(II) as metal nodes,[27−29] and the coordination polymers prepared exhibit exceptional abilities for selective CO_2 absorption and drug delivery. On the other hand, adenine's multiple Lewis basic sites, an amino group, and pyrimidine nitrogen atoms make it possible to create a photoinduced electron transfer (PET) sensory system *via* linking a fluorophore. Pioneering work on the use of adenine as an effective receptor for the construction of fluorescent PET sensors has been done by Ghosh and coworkers.[30−32] In their reported sensors, adenine was connected to an anthracnce molecule *via* a spacer, and the decreased fluorescence of anthracnce can be observed when the coordination between analytes and adenine occurred. The adenine-based fluorescent PET sensors have been used for the selective detection of dicarboxylic acids, iodide, and Cu^{2+}.[30−32] PET is an often-used mechanism of fluorescence sensing, which has been applied in the design of many fluorescent sensors based on a fluorescence off/on strategy. However, most of the fluorescent PET sensors were constructed by using conventional fluorescence molecules; very few examples of nanomaterials were reported.

In this work, we attempt to utilize the highly tailorable property of coordination polymers to design and prepare a kind of lanthanide coordination polymer nanoparticles (CPNPs) with PET fluorescence sensing function and use this nanosensor to detect Hg^{2+} in aqueous solution. The lanthanide CPNPs were composed of adenine (Ad), terbium ion (Tb^{3+}), and dipicolinic acid (DPA), denoted as Ad/Tb/DPA CPNPs. The chemical structures of Ad and DPA are displayed in Figure S1. As stated above, the adenine can coordinate to Tb^{3+} to form a coordination polymer. DPA is an aromatic dicarboxylic acid, which can not only offer its O atoms of carboxylic acid groups and N atom of the aromatic ring for the coordination of Tb^{3+} but also transfer its absorbed energy to Tb^{3+} to sensitize the fluorescence of Tb^{3+}. Because the coordination ability of the O atom to Tb^{3+} is stronger than that of the N atom,[33] the coordination of Tb^{3+} with DPA may mainly occur. Thus, the adenine might provide its Hoogsteen binding (HG) site for the binding of one of carboxylic acid group in DPA by hydrogen bonds,[30] forming an Ad-Tb^{3+}-DPA coordination network. Under light excitation, the nitrogen atom of adenine may transfer its electron to DPA and prevent the intramolecular energy transfer from DPA to Tb^{3+}, leading to the quench of fluorescence of Ad/Tb/DPA CPNPs. Mercury ions (Hg^{2+}) have a high affinity to N atoms, which has been often used to disrupt the PET process.[34,35] In the presence of Hg^{2+}, therefore, an enhanced fluorescence of Ad/Tb/DPA CPNPs by the coordination of Hg^{2+} with adenine would be observed (Scheme 1).

RESULTS AND DISCUSSION

The CPNPs constructed from Tb^{3+}, adenine, and DPA, Ad/Tb/DPA CPNPs, were synthesized by a solvothermal

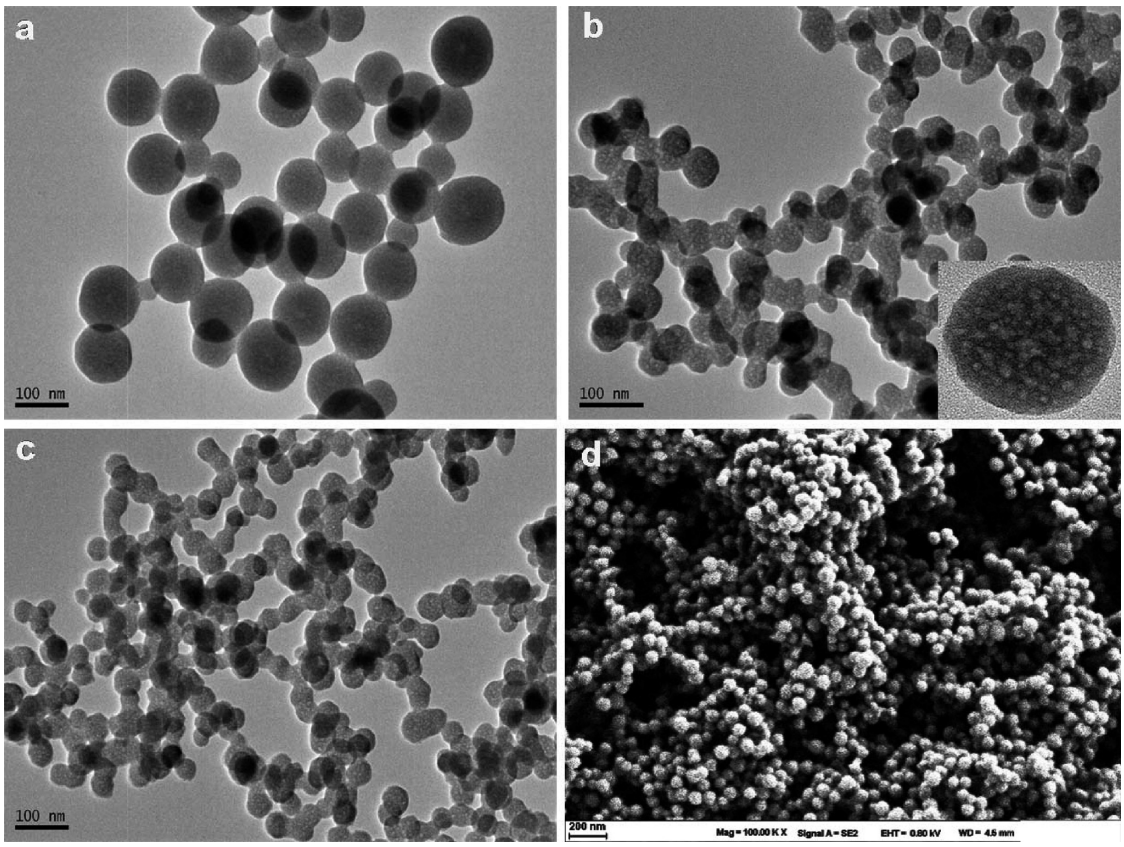

Figure 1. TEM images of coordination polymer nanoparticles of Ad/Tb (a), Ad/Tb/DPA (b), and Ad/Tb/DPA in the presence of Hg^{2+} (c) and SEM image of Ad/Tb/DPA (d).

reaction.[36] As a control, CPNPs consisting of Tb^{3+} and adenine, Ad/Tb CPNPs, were prepared under the same conditions. Compared with pure adenine, the changes of Ad/Tb CPNPs in the FTIR spectrum confirm the coordination of adenine to Tb^{3+} (Figure S2). The morphology of these lanthanide CPNPs was examined by transmission electron microscopy (TEM) and scanning electron microscopy (SEM). As shown in Figure 1, all the CPNPs are spherical. The selected area electron diffraction (SAED) image of the lanthanide CPNPs indicated they are amorphous (Figure S3). In the presence of DPA, the average size of the Ad/Tb CPNPs decreased from 100 ± 4 nm to approximately 45 ± 3 nm (Figure S4), and the particles seem more adherent. This may be due to the interactions of DPA and Tb^{3+} on the surface of the nanoparticle. By careful observation, it can be seen that many pores are distributed on the nanoparticles, which became clear with the addition of DPA. This supports that the introduction of auxiliary linking molecules containing carboxylic acid groups can promote the formation of larger accessible pores during the synthesis of metal–organic coordination polymers.[27] The chemical compositions of the CPNPs were determined by an energy-dispersed spectrum (EDS) (Figure S5). The peaks of Tb, C, N, H, and O were found (other peaks originated from the Si substrate), revealing that Tb^{3+}, adenine, and DPA were involved in the formation of the CPNPs.

As shown in Figure 2, no fluorescence was observed from Ad/Tb CPNPs, which is due to the low molar absorption coefficient of Tb^{3+}. Ad/Tb/DPA CPNPs are weakly fluorescent; there was an excitation peak at 270 nm and emission peaks at 490, 545, 584, and 620 nm in the spectra of Ad/Tb/DPA CPNPs. The positions of these excitation and emission peaks of Ad/Tb/DPA CPNPs are the same as that of complex DPA-Tb, which is strongly fluorescent in aqueous solution. The excitation peak at 270 nm resulted from the absorption of DPA, whereas the peaks at 490, 545, 584, and 620 nm are the typical emission of Tb^{3+}, which implies that DPA molecules were combined into Ad/Tb/DPA CPNPs and that the emission of Tb^{3+} resulted from an intramolecular energy transfer from DPA to Tb^{3+}. In the presence of Hg^{2+}, however, the weak fluorescence of Ad/Tb/DPA CPNPs was enhanced significantly (approximately 5-fold). This may be because the PET process from adenine to DPA was suppressed by Hg^{2+}.

To discern the coordination interaction between adenine and DPA, we conducted an FTIR analysis. Figure S6 is the FTIR spectra of the CPNPs of Ad/Tb, Ad/Tb/DPA, and Ad/Tb/DPA in the presence of Hg^{2+}, respectively. Compared with Ad/Tb, the shifts of the FTIR spectra of Ad/Tb/DPA in the C5–N7 stretching vibrations (from 756 to 725 cm^{-1} and from 1054 to 1075 cm^{-1}), NH_2 scissoring vibration (from 1385 to

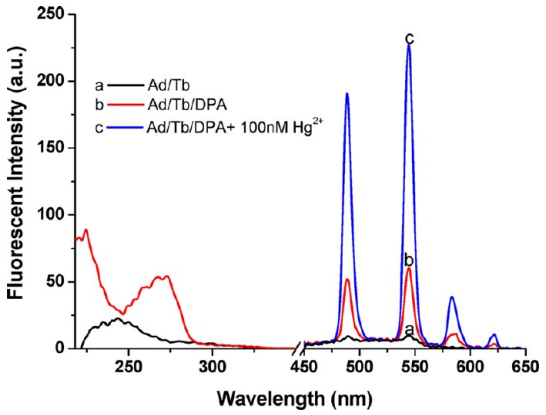

Figure 2. Excitation and emission spectra of Ad/Tb CPNPs (a) and Ad/Tb/DPA CPNPs (b). (c) Emission spectrum of Ad/Tb/DPA CPNPs in the presence of 100 nM Hg^{2+}. The 260 and 270 nm excitation wavelengths were used for the emission spectra of Ad/Tb CPNPs and Ad/Tb/DPA CPNPs, respectively.

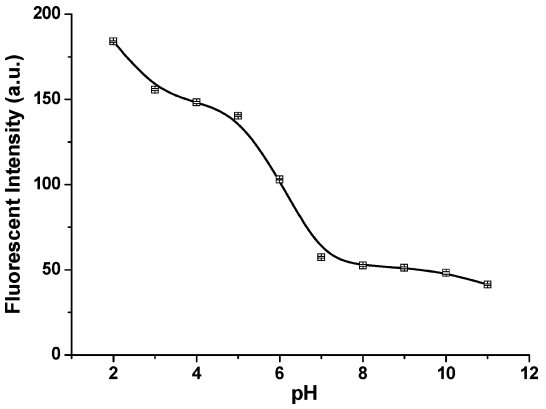

Figure 3. Changes in the fluorescence intensity of Ad/Tb/DPA CPNPs with different pH in HEPES buffer.

1396 cm^{-1}), and N7−C8 stretching vibrations (from 1517 to 1519 cm^{-1}) suggest that there was a interaction between DPA and adenine's N7 and NH_2 sites.[25,37] This is consistent with the fact that the HG site of adenine prefers to bind an aromatic acid.[30] The binding of adenine with DPA decreased the intramolecular energy transfer from DPA to Tb^{3+}, leading to the quenching of DPA-Tb fluorescence. The typical characteristic of the PET mechanism is that the fluorescence accompanying the PET process increases with the decrease of the pH value of the solution.[38,39] As exhibited in Figure 3, the fluorescence intensity of Ad/Tb/DPA CPNPs increased with the decrease of pH, indicating this is a PET behavior between adenine and DPA. In the acidic condition, the protonation of adenine and DPA deactivated the PET process, leading to the recovery of the energy transfer process from DPA to Tb^{3+} and then a fluorescence enhancement of Ad/Tb/DPA CPNPs. Furthermore, the pH of the solution showed influences on stability of Ad/Tb/DPA CPNPs. When the pH value of the solution is less than 4, TEM showed that Ad/Tb/DPA CPNPs became gradually dissociated due to the protonation of the ligands, and the dissociation increased with the acidity of the solution (data not shown). However, when the pH value of the solution reached or exceeded 6, Ad/Tb/DPA CPNPs are stable even if stored for several months. In this work, a Hg^{2+}-induced enhancement reaction was carried out in aqueous solution with neutral pH.

Hg^{2+} is an effective quencher for the DPA-Tb complex with strong fluorescence in aqueous solution because of its more stable binding to DPA than that of Tb^{3+}, leading to a replacement of Tb^{3+} in the complex by Hg^{2+}.[40] But here, the presence of Hg^{2+} enhanced the fluorescence of CPNPs. This indicated that Hg^{2+} was not directly bound to the DPA molecule alone, but bound to Ad molecules. The binding of Hg^{2+} to Ad interrupted the PET process to result in a fluorescence enhancement of CPNPs. The Hg^{2+}-induced fluorescence quenching usually causes a decrease of fluorescence lifetime of lanthanide ions.[41] After the addition of Hg^{2+}, EDS analysis confirmed that Ad/Tb/DPA CPNPs contain Hg^{2+} ions (Figure S5c), but the fluorescence lifetime of Tb^{3+} is almost not changed (Figure S7). This further indicates that the inherent transition processes of Tb^{3+} induced by the ligand field are not affected by Hg^{2+}. So we speculate that the coordination of Hg^{2+} mainly occurred with the adenine nitrogen, although the anion nature of the Ad/Tb/DPA CPNPs from DPA may also contribute to the bonding of Hg^{2+}.[27]

To verify the binding sites of Hg^{2+} with Ad/Tb/DPA CPNPs, the FTIR spectra of Ad/Tb/DPA CPNPs were compared in the absence and presence of Hg^{2+}. From Figure S6, we found that the wavenumbers in the C−N stretching vibration and NH_2 scissoring vibration of adenine in Ad/Tb/DPA CPNPs were shifted from 1075 and 1396 cm^{-1} to 1090 and 1384 cm^{-1}, respectively, in the presence of Hg^{2+}, indicating the coordination of Hg^{2+} with the N atoms of adenine.[37] Meanwhile, the wavenumber in the carboxyl asymmetric vibration of DPA shifted from 1699 cm^{-1} to 1623 cm^{-1} reflects the interaction of carboxylic acid group of DPA with Hg^{2+}.[42] Therefore, we attribute the fluorescent enhancement of Ad/Tb/DPA CPNPs to the coordination of Hg^{2+} with adenine nitrogen. The formation of the Hg-Ad/Tb/DPA complex suppressed the intramolecular PET from the adenine nitrogen to DPA, which results in fluorescence enhancement.

The fluorescent behavior of Ad/Tb/DPA CPNPs was also confirmed by the centrifugation experiment (Figure S8). After centrifugation, the supernatants of aqueous Ad/Tb/DPA CPNPs are nonfluorescent and only the centrifuged sediment with Hg^{2+} is fluorescent under a usual UV lamp (Figure S8a). Furthermore, the centrifuged sediments in the presence of different concentrations of Hg^{2+} were collected by spin columns with membrane filtration. The color of the membranes can be observed by the naked eye under a usual UV lamp, and their brightness increased with the concentration of Hg^{2+} (Figure S8b). These results suggest that Hg^{2+}-enhanced fluorescence is from Ad/Tb/DPA CPNPs themselves.

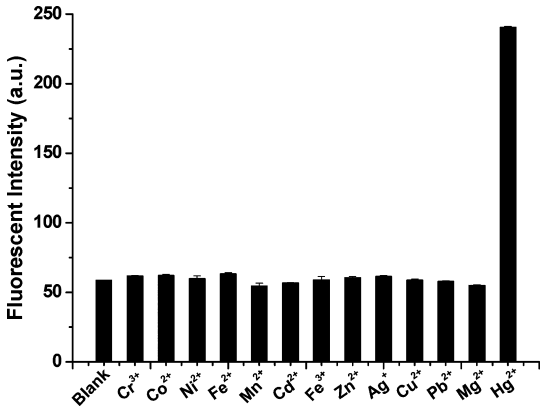

Figure 4. Effect of various metal ions (1 μM) on the fluorescence intensity of Ad/Tb/DPA CPNPs at 545 nm.

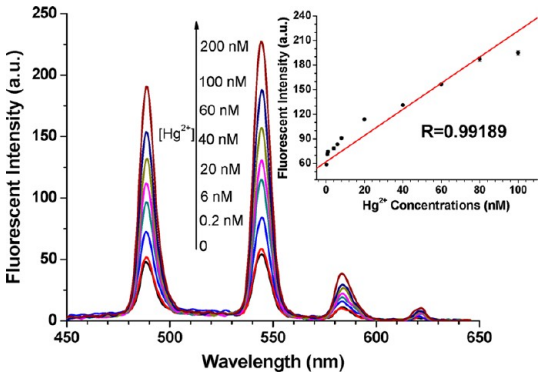

Figure 5. Fluorescence emission spectra of Ad/Tb/DPA CPNPs in the presence of different concentrations of Hg^{2+} solution (0, 0.2, 6, 20, 40, 60, 100, 200 nM). Inset: Linear relationship between the fluorescence intensity of Ad/Tb/DPA CPNPs at 545 nm and Hg^{2+} concentration.

We examined the effect of other metal ions on the fluorescence intensity of Ad/Tb/DPA CPNPs under identical conditions. As shown in Figure 4, only the addition of Hg^{2+} resulted in a significant fluorescence enhancement; no remarked changes in the fluorescence of Ad/Tb/DPA CPNPs were observed upon the addition of other metal ions, including Cr^{3+}, Co^{2+}, Ni^{2+}, Fe^{2+}, Mn^{2+}, Cd^{2+}, Fe^{3+}, Zn^{2+}, Ag^{+}, Cu^{2+}, Pb^{2+}, and Mg^{2+}. To further evaluate the selectivity of Ad/Tb/DPA CPNPs to Hg^{2+}, we carried out the measurements in the presence of mixed metal ions (Figure S9). The results indicated that all the coexisting metal ions produced negligible interferences in comparison with Hg^{2+}. The high selectivity of Ad/Tb/DPA CPNPs to Hg^{2+} is ascribed to the fact that Hg^{2+} possesses a much higher binding ability to the N atoms of adenine[43,44] and the carboxylic acid group of DPA than other metal ions, and the stability constant of the Hg^{2+} ion with DPA is approximately 3 orders of magnitude higher than that of other ions.[40]

The unusual selectivity of Ad/Tb/DPA CPNPs to Hg^{2+} prompted us to apply it to the detection of trace Hg^{2+} in environmental water samples. The Hg^{2+}-induced fluorescence enhancement was fast and reached a maximum within 5 min (Figure S10). The fluorescence response of Ad/Tb/DPA CPNPs to Hg^{2+} with different concentrations is shown in Figure 5. The fluorescence of Ad/Tb/DPA CPNPs was enhanced gradually with the increase of Hg^{2+} concentrations from 0 to 200 nM. There is a linear fluorescence response to Hg^{2+} in the concentration range 0.2−100 nM. The detection limit is 0.2 nM on the basis of a signal-to-noise ratio of 3:1. This detection limit not only is much lower than most of the previously reported fluorescence probes for Hg^{2+},[35,41,45,46] but also satisfies the maximum permitted level of 10 nM Hg^{2+} in drinking water regulated by the U.S. Environmental Protection Agency (EPA).[47] It is important to monitor the level of inorganic Hg^{2+} in water samples, as Hg^{2+} can be converted to hypertoxic methylmercury by the food chain and accumulated in higher organisms, especially in large edible fish. The water samples spiked with different concentrations of Hg^{2+} were determined by employing Ad/Tb/DPA CPNPs. As seen from Table S1, the added standard Hg^{2+} can be accurately measured with good recoveries (more than 96%), indicating that Ad/Tb/DPA CPNPs can be used to monitor Hg^{2+} in water samples, and this method has no obvious system error of detection.

CONCLUSION

In summary, we have prepared adenine-based lanthanide CPNPs with desired function. We also showed the potential application of Ad/Tb/DPA CPNPs as fluorescence sensors for the detection of Hg^{2+}, which is based on the suppression of the intramolecular PET process from adenine to DPA. As a sensor for the detection of Hg^{2+}, Ad/Tb/DPA CPNPs exhibited excellent selectivity and ultrahigh sensitivity up to the 0.2 nM detection limit. Ad/Tb/DPA CPNPs also possess a long enough fluorescence lifetime for time-resolved fluorescence assays due to the inclusion of Tb^{3+} ions. This is especially advantageous for the detection of biosamples with autofluorescence. To the best of our knowledge, this is the first Hg^{2+}-sensitive coordination polymer nanoparticle sensor based on the fluorescence PET mechanism. We believe that the present synthetic strategy constructing special functions from initial building blocks can be extended to the preparation of other lanthanide CPNP-based fluorescent probes for wide applications in biosensing, imaging, drug delivery, and so on.

METHODS

Chemicals and Solutions. Terbium nitrate (99.99%) was purchased from Baotou Rewin Rare Earth Metal Materials Co., Ltd.; 2,6-pyridinedicarboxylic acid (99%, dipicolinic acid) was purchased from Sigma-Aldrich; adenine and metal salts ($AgNO_3$, $MgCl_2$, $Pb(NO_3)_2$, $Zn(NO_3)_2$, $CdCl_2$, $FeCl_3$, $FeCl_2$, $NiCl_2$, $CoCl_2$,

$MnCl_2$, $CrCl_3$, and $CuCl_2$) were purchased from Sinopharm Chemical Reagent Company. Mercury(II) nitrate was from Beijing Zhongbiao Huawei Technology Company. *N*-2-Hydroxyethylpiperazine-*N*′-2-ethanesulfonic acid (HEPES) was obtained from Sangon Biotech (Shanghai) Co., Ltd.; ultrapure water (18 MΩ cm; Milli-Q, Millipore) was used for the preparation of all aqueous solutions. HEPES buffer (100 mM, pH 7.4) was prepared by dissolving appropriate amounts of HEPES in water and adjusting to pH 7.4 with 10 M NaOH. The stock solutions of interference ions (10 mM) were prepared by dissolving $AgNO_3$, $MgCl_2$, $Pb(NO_3)_2$, $CdCl_2$, $FeCl_3$, $FeCl_2$, $NiCl_2$, $CoCl_2$, $MnCl_2$, $CrCl_3$, $CuCl_2$, and $Zn(NO_3)_2$ in water, respectively. Unless otherwise stated, all chemicals are of analytical reagent grade and were used without further purification.

Instruments. The morphology of CPNPs prepared was observed by transmission electron microscopy (JEM-2100, Japan) and scanning electron microscopy (Carl Zeiss Ultra Plus, Germany). Energy dispersive spectra were recorded on an X-Max (Oxford, UK) energy dispersive spectrometer. Fluorescence spectra and emission intensity were recorded on an LS55 luminescence spectrometer (PerkinElmer, UK). The detection solution was placed in a quartz microcuvette with 100 μL capacity and 2 mm light path. The 270 nm excitation wavelength was used for the emission spectra. A delay time of 0.05 ms and a gate time of 2 ms were used. Excitation spectra were recorded by observing the emission intensity of Tb^{3+} at 545 nm. For the emission lifetime, the fluorescence intensities at 545 nm were recorded under different delay times and fitted with an exponential function. UV−visible absorption spectra were recorded with a UV-3150 spectrophotometer (Shimadzu, Japan). Fourier transform infrared spectra (FTIR) were recorded with an Avatar 360 FTIR spectrometer (Nicolet, USA). All the experiments were performed at room temperature.

Preparation of Ad/Tb/DPA and Ad/Tb Coordination Polymer Nanoparticles. The Ad/Tb/DPA coordination polymer nanoparticles were prepared on the basis of the previous method.[36] Typically, 2 mL of adenine aqueous solution (20 mM) and 0.5 mL of DPA aqueous solution (10 mM) were added to 8 mL of DMF and mixed well. Then 2 mL of $Tb(NO_3)_3$ aqueous solution (40 mM) was added to the above solution under stirring. The total reaction volume was 12.5 mL, and the final concentrations of adenine, DPA, and Tb^{3+} were 3.2, 0.4, and 6.4 mM, respectively. After stirring 20 min, the transparent solution was sealed in a Teflon-lined autoclave, heated at 150 °C for 2 h, and then cooled to room temperature naturally. The white precipitate was collected by centrifugation at 13 000 rpm for 10 min. To remove unreacted reactants, we washed the precipitate three times with absolute ethanol. Finally, the precipitate (approximately 0.0265 g, dry) was dispersed in 2 mL of pure water to form a CNCP suspension for use. As a control experiment, Ad/Tb CPNPs were synthesized by the same experimental steps and conditions mentioned above except replacing DPA by 0.5 mL of H_2O.

Fluorescence Response of Ad/Tb/DPA CPNPs to Hg^{2+} in Aqueous Solution. The original Ad/Tb/DPA CPNPs suspension was diluted 50-fold for the detection of Hg^{2+} in aqueous solution. For the sensitivity experiments, different volumes of Hg^{2+} solution with concentrations from 0 to 400 nM were added to 3 μL of an Ad/Tb/DPA CPNP suspension, and H_2O was added until the total volume reached 100 μL. After reacting for 5 min, the fluorescence spectra were recorded using an excitation wavelength of 270 nm. To test the selectivity of Ad/Tb/DPA CPNPs to Hg^{2+}, 1 μL of 10 mM stock solutions of these interference ions were added to 3 μL of an Ad/Tb/DPA CPNPs suspension, respectively. The total volume reached 100 μL by adding pure water. The reaction lasted 5 min before measuring the fluorescence intensities of these mixtures at 545 nm. For the effect of pH on the fluorescence intensity of the CPNPs, 3 μL of Ad/Tb/DPA CPNPs suspension was added to 97 μL of HEPES buffer with different pH values, respectively. The mixture was shaken well and reacted for 5 min before recording the fluorescence intensities.

Determination of Hg^{2+} in Water Samples. The water samples were collected from drinking water and tap water. A series of water samples containing different concentrations of Hg^{2+} were prepared by "spiking" them with standard solutions of Hg^{2+}. These water samples were added to 3 μL of Ad/Tb/DPA CPNP solutions, respectively, and incubated for 5 min. The fluorescence intensities at 545 nm were recorded under a 270 nm excitation wavelength.

Conflict of Interest: The authors declare no competing financial interest.

Acknowledgment. This work was supported by the Natural Science Foundation of China (60671014, 20775012) and the Scientific Research Foundation of Graduate School of Southeast University (YBJJ1118).

Supporting Information Available: Figures S1−10, Table S1. This information is available free of charge *via* the Internet at http://pubs.acs.org.

REFERENCES AND NOTES

1. Della Rocca, J.; Liu, D.; Lin, W. Nanoscale Metal-Organic Frameworks for Biomedical Imaging and Drug Delivery. *Acc. Chem. Res.* **2011**, *44*, 957–968.
2. Cui, Y.; Yue, Y.; Qian, G.; Chen, B. Luminescent Functional Metal-Organic Frameworks. *Chem. Rev.* **2012**, *112*, 1126–1162.
3. Li, J.-R.; Kuppler, R. J.; Zhou, H.-C. Selective Gas Adsorption and Separation in Metal-Organic Frameworks. *Chem. Soc. Rev.* **2009**, *38*, 1477–1504.
4. Suh, M. P.; Park, H. J.; Prasad, T. K.; Lim, D.-W. Hydrogen Storage in Metal-Organic Frameworks. *Chem. Rev.* **2012**, *112*, 782–835.
5. Park, K. H.; Jang, K.; Son, S. U.; Sweigart, D. A. Self-Supported Organometallic Rhodium Quinonoid Nanocatalysts for Stereoselective Polymerization of Phenylacetylene. *J. Am. Chem. Soc.* **2006**, *128*, 8740–8741.
6. Cunha-Silva, L.; Lima, S.; Ananias, D.; Silva, P.; Mafra, L.; Carlos, L. D.; Pillinger, M.; Valente, A. A.; Almeida Paz, F. A.; Rocha, J. Multi-functional Rare-Earth Hybrid Layered Networks: Photoluminescence and Catalysis Studies. *J. Mater. Chem.* **2009**, *19*, 2618–2632.
7. Chen, B.; Xiang, S.; Qian, G. Metal-Organic Frameworks with Functional Pores for Recognition of Small Molecules. *Acc. Chem. Res.* **2010**, *43*, 1115–1124.
8. Wu, P.; Wang, J.; Li, Y.; He, C.; Xie, Z.; Duan, C. Luminescent Sensing and Catalytic Performances of a Multifunctional Lanthanide-Organic Framework Comprising a Triphenylamine Moiety. *Adv. Funct. Mater.* **2011**, *21*, 2788–2794.
9. Liu, D.; Huxford, R. C.; Lin, W. Phosphorescent Nanoscale Coordination Polymers as Contrast Agents for Optical Imaging. *Angew. Chem., Int. Ed.* **2011**, *50*, 3696–3700.
10. Nishiyabu, R.; Hashimoto, N.; Cho, T.; Watanabe, K.; Yasunaga, T.; Endo, A.; Kaneko, K.; Niidome, T.; Murata, M.; Adachi, C.; *et al.* Nanoparticles of Adaptive Supramolecular Networks Self-Assembled from Nucleotides and Lanthanide Ions. *J. Am. Chem. Soc.* **2009**, *131*, 2151–2158.
11. Della Rocca, J.; Lin, W. Nanoscale Metal-Organic Frameworks: Magnetic Resonance Imaging Contrast Agents and Beyond. *Eur. J. Inorg. Chem.* **2010**, *2010*, 3725–3734.
12. Oh, M.; Mirkin, C. A. Ion Exchange as a Way of Controlling the Chemical Compositions of Nano- and Microparticles Made from Infinite Coordination Polymers. *Angew. Chem., Int. Ed.* **2006**, *45*, 5492–5494.
13. Rieter, W. J.; Pott, K. M.; Taylor, K. M. L.; Lin, W. Nanoscale Coordination Polymers for Platinum-Based Anticancer Drug Delivery. *J. Am. Chem. Soc.* **2008**, *130*, 11584–11585.
14. Imaz, I.; Rubio-Martinez, M.; Garcia-Fernandez, L.; Garcia, F.; Ruiz-Molina, D.; Hernando, J.; Puntes, V.; Maspoch, D. Coordination Polymer Particles as Potential Drug Delivery Systems. *Chem. Commun.* **2010**, *46*, 4737–4739.
15. Xu, H.; Liu, F.; Cui, Y.; Chen, B.; Qian, G. A Luminescent Nanoscale Metal-Organic Framework for Sensing of Nitroaromatic Explosives. *Chem. Commun.* **2011**, *47*, 3153–3155.
16. Tan, H.; Chen, Y. Ag^{+}-Enhanced Fluorescence of Lanthanide/Nucleotide Coordination Polymers and Ag^{+} Sensing. *Chem. Commun.* **2011**, *47*, 12373–12375.
17. Yang, W.; Feng, J.; Zhang, H. Facile and Rapid Fabrication of Nanostructured Lanthanide Coordination Polymers as

Selective Luminescent Probes in Aqueous Solution. *J. Mater. Chem.* **2012**, *22*, 6819–6823.
18. Spokoyny, A. M.; Kim, D.; Sumrein, A.; Mirkin, C. A. Infinite Coordination Polymer Nano- and Microparticle Structures. *Chem. Soc. Rev.* **2009**, *38*, 1218–1227.
19. Lin, W.; Rieter, W. J.; Taylor, K. M. L. Modular Synthesis of Functional Nanoscale Coordination Polymers. *Angew. Chem., Int. Ed.* **2009**, *48*, 650–658.
20. Imaz, I.; Rubio-Martinez, M.; An, J.; Sole-Font, I.; Rosi, N. L.; Maspoch, D. Metal-Biomolecule Frameworks (MBioFs). *Chem. Commun.* **2011**, *47*, 7287–7302.
21. Nishiyabu, R.; Aimé, C.; Gondo, R.; Noguchi, T.; Kimizuka, N. Confining Molecules within Aqueous Coordination Nanoparticles by Adaptive Molecular Self-Assembly. *Angew. Chem., Int. Ed.* **2009**, *48*, 9465–9468.
22. Aimé, C.; Nishiyabu, R.; Gondo, R.; Kimizuka, N. Switching On Luminescence in Nucleotide/Lanthanide Coordination Nanoparticles via Synergistic Interactions with a Cofactor Ligand. *Chem.—Eur. J.* **2010**, *16*, 3604–3607.
23. Aimé, C.; Nishiyabu, R.; Gondo, R.; Kaneko, K.; Kimizuka, N. Controlled Self-Assembly of Nucleotide-Lanthanide Complexes: Specific Formation of Nanofibers from Dimeric Guanine Nucleotides. *Chem. Commun.* **2008**, *44*, 6534–6536.
24. Purohit, C. S.; Verma, S. A Luminescent Silver-Adenine Metallamacrocyclic Quartet. *J. Am. Chem. Soc.* **2006**, *128*, 400–401.
25. Wei, H.; Li, B.; Du, Y.; Dong, S.; Wang, E. Nucleobase-Metal Hybrid Materials: Preparation of Submicrometer-Scale, Spherical Colloidal Particles of Adenine-Gold(III) via a Supramolecular Hierarchical Self-Assembly Approach. *Chem. Mater.* **2007**, *19*, 2987–2993.
26. Mishra, A. K.; Kumar, J.; Khanna, S.; Verma, S. Crystallographic Signatures of Cobalt Coordination with Modified Adenine Nucleobase Containing Carboxyl Group Pendants. *Cryst. Growth. Des.* **2011**, *11*, 1623–1630.
27. An, J.; Geib, S. J.; Rosi, N. L. Cation-Triggered Drug Release from a Porous Zinc-Adeninate Metal-Organic Framework. *J. Am. Chem. Soc.* **2009**, *131*, 8376–8377.
28. An, J.; Shade, C. M.; Chengelis-Czegan, D. A.; Petoud, S. p.; Rosi, N. L. Zinc-Adeninate Metal-Organic Framework for Aqueous Encapsulation and Sensitization of Near-infrared and Visible Emitting Lanthanide Cations. *J. Am. Chem. Soc.* **2011**, *133*, 1220–1223.
29. An, J.; Geib, S. J.; Rosi, N. L. High and Selective CO_2 Uptake in a Cobalt Adeninate Metal-Organic Framework Exhibiting Pyrimidine- and Amino-Decorated Pores. *J. Am. Chem. Soc.* **2009**, *132*, 38–39.
30. Ghosh, K.; Sen, T.; Fröhlich, R. Adenine-based Receptor for Dicarboxylic Acids. *Tetrahedron Lett.* **2007**, *48*, 7022–7026.
31. Ghosh, K.; Sen, T. Adenine-based Urea Receptors in Fluorescent Recognition of Iodide. *Tetrahedron Lett.* **2008**, *49*, 7204–7208.
32. Ghosh, K.; Sen, T. Anthracene Coupled Adenine for the Selective Sensing of Copper Ions. *Beilstein J. Org. Chem.* **2010**, *6*, 44–51.
33. Richardson, F. S. Terbium(III) and Europium(III) Ions as Luminescent Probes and Stains for Biomolecular Systems. *Chem. Rev.* **1982**, *82*, 541–552.
34. Nolan, E. M.; Lippard, S. J. A "Turn-On" Fluorescent Sensor for the Selective Detection of Mercuric Ion in Aqueous Media. *J. Am. Chem. Soc.* **2003**, *125*, 14270–14271.
35. Bhalla, V.; Tejpal, R.; Kumar, M.; Puri, R. K.; Mahajan, R. K. Terphenyl Based `Turn On' Fluorescent Sensor for Mercury. *Tetrahedron Lett.* **2009**, *50*, 2649–2652.
36. Zhong, S.-L.; Xu, R.; Zhang, L.-F.; Qu, W.-G.; Gao, G.-Q.; Wu, X.-L.; Xu, A.-W. Terbium-based Infinite Coordination Polymer Hollow Microspheres: Preparation and White-Light Emission. *J. Mater. Chem.* **2011**, *21*, 16574–16580.
37. Nowak, M. J.; Lapinski, L.; Kwiatkowski, J. S.; Leszczyński, J. Molecular Structure and Infrared Spectra of Adenine. Experimental Matrix Isolation and Density Functional Theory Study of Adenine 15N Isotopomers. *J. Phys. Chem.* **1996**, *100*, 3527–3534.
38. Guo, X.; Qian, X.; Jia, L. A Highly Selective and Sensitive Fluorescent Chemosensor for Hg^{2+} in Neutral Buffer Aqueous Solution. *J. Am. Chem. Soc.* **2004**, *126*, 2272–2273.
39. Zong, G.; Lu, G. An Anthracene-Based Chemosensor for Multiple Logic Operations at the Molecular Level. *J. Phys. Chem. C* **2009**, *113*, 2541–2546.
40. Norkus, E.; Stalnionienė, I.; Crans, D. C. Interaction of Pyridine- and 4-Hydroxypyridine-2,6-Dicarboxylic Acids with Heavy Metal Ions in Aqueous Solutions. *Heteroat. Chem.* **2003**, *14*, 625–632.
41. Tan, H.; Zhang, Y.; Chen, Y. Detection of Mercury Ions (Hg^{2+}) in Urine Using a Terbium Chelate Fluorescent Probe. *Sens. Actuators B: Chem.* **2011**, *156*, 120–125.
42. An, B.-L.; Shi, J.-X.; Wong, W.-K.; Cheah, K.-W.; Li, R.-H.; Yang, Y.-S.; Gong, M.-L. Synthesis and Luminescence of a Novel Conjugated Europium Complex with 6-Parachloroaniline Carbonyl 2-Pyridine Carboxylic Acid. *J. Lumin.* **2002**, *99*, 155–160.
43. Cotton, F. A.; Wilkinson, G.; Murillo, C. A.; Bochmann, M. *Advanced Inorganic Chemistry*, 6th ed.; John Wiley & Sons, Inc., 1999.
44. Phillips, R. Adenosine and the Adenine Nucleotides. Ionization, Metal Complex Formation, and Conformation in Solution. *Chem. Rev.* **1966**, *66*, 501–527.
45. Liu, D.; Qu, W.; Chen, W.; Zhang, W.; Wang, Z.; Jiang, X. Highly Sensitive, Colorimetric Detection of Mercury(II) in Aqueous Media by Quaternary Ammonium Group-Capped Gold Nanoparticles at Room Temperature. *Anal. Chem.* **2010**, *82*, 9606–9610.
46. Xue, X.; Wang, F.; Liu, X. One-Step, Room Temperature, Colorimetric Detection of Mercury (Hg^{2+}) Using DNA/Nanoparticle Conjugates. *J. Am. Chem. Soc.* **2008**, *130*, 3244–3245.
47. EPA, U.S. *Drinking Water Criteria Document for Inorganic Mercury*; Environmental Criteria and Assessment Office: Cincinnati, OH, **1988**.